RSC Advances

ROYAL SOCIETY OF CHEMISTRY

PAPER

View Article Online
View Journal | View Issue

Check for updates

Cite this: *RSC Adv.*, 2020, **10**, 18082

Structural studies of two capsaicinoids: dihydrocapsaicin and nonivamide. ^{13}C and ^{15}N MAS NMR supported by genetic algorithm and GIAO DFT calculations

Paweł Siudem, *[a] Jarosław Bukowicki,[a] Iwona Wawer[b] and Katarzyna Paradowska[a]

Received 11th February 2020
Accepted 29th April 2020

DOI: 10.1039/d0ra01320j

rsc.li/rsc-advances

Capsaicinoids are alkaloid type capsaicin analogs with prospective pharmacological activity. However their solid state conformations have not been studied yet. As part of the study, cross polarization (CP) magic angle spinning (MAS) solid state ^{13}C and ^{15}N NMR spectra of dihydrocapsaicin (DHCAP) and nonivamide (NVA) were recorded. Solid state chemical shifts differ from their solution counterparts; remarkable differences occur for carbons C2′, C6′ and C7′ linked to C1′ in DHCAP and with methylene carbons C4–C8 in NVA. The doubling of some resonances in the spectra of solid NVA indicates that there are two molecules in the crystallographic asymmetric unit. DFT GIAO calculations of shielding constants were performed for several geometric isomers, including molecules with different orientations of aliphatic chain with respect to aromatic ring. Low-energy conformers were found by genetic algorithm methodology. Comparison of experimental ^{13}C chemical shifts with theoretical (GIAO DFT) shielding parameters was helpful in predicting the most reliable geometry in the solid state. Cross polarization time constants T_{CP} and relaxation times in the rotating frame $T_{1\rho}^{H}$ were obtained from variable-contact cross-polarization experiments. $T_{1\rho}^{H}$ are longer in the order: NVA < CAP < DHCAP.

Introduction

Capsaicin (8-methyl-*N*-vanillyl-6-nonenamide) is a pungent alkaloid found in chili pepper fruit. Over the last decades, it has been described as a multipotent bioactive compound.[1] According to these studies, many new capsaicin analogs with expected biological activity were sought. Nonivamide (NVA) and dihydrocapsaicin (DHCAP) (Fig. 1) are two derivatives of capsaicin (CAP)[2,3] which can be found as a component of analgesic drugs or pepper spray;[4] they are also used in pain-killer cream and patches.

Pharmacological properties of potential drug substances, crucial for modern pharmaceutical sciences, are widely studied using spectroscopic and theoretical methods. The biological activity of a compound defined by the affinity of a small-molecule ligand towards the macromolecular receptor can be explored using *in silico* methods, like the molecular docking approach. The docking process involves prediction of multiple structural conformations in a binding pocket as a basic step. However, solid state conformation analysis is also very important, because the majority of dosage forms are solid dosage forms and solid state conformation is connected with pharmacokinetic properties of an API (Active Pharmaceutical Ingredient). Therefore, low energy conformations of capsaicinoids, as well as their solid-state structure are of interest and should be studied in detail.

Crystallographic data for nonivamide and dihydrocapsaicin do not exist. Since all our attempts to obtain single crystals of capsaicinoids suitable for XRD measurement have been unsuccessful, solid-state NMR is proposed as a method for structure determination for these substances. NMR spectroscopy supported by theoretical calculations was used as the main method of structural studies. This approach was previously applied by us in the study on capsaicin structure[5] and the results were compared with PXRD data. To the best of our knowledge, this work is the first to focus on the solid-state structure of nonivamide and dihydrocapsaicin. Our results may be a step towards determination of the conformation – bioavailability relationship, because neither the conformations nor the crystal structures of these capsaicinoids have been described before.

Methods

Materials

NVA (nonivamide) and DHCAP (dihydrocapsaicin) were purchased from Sigma-Aldrich (Aldrich no. V9130 and M1022 respectively).

[a]*Department of Physical Chemistry, Faculty of Pharmacy, Medical University of Warsaw, Banacha 1, PL-02097 Warsaw, Poland. E-mail: pawel.siudem@wum.edu.pl; Fax: +48 22 5720 950; Tel: +48 22 5720 950*

[b]*The State Higher Vocational School, Rynek 1, PL-38400 Krosno, Poland*

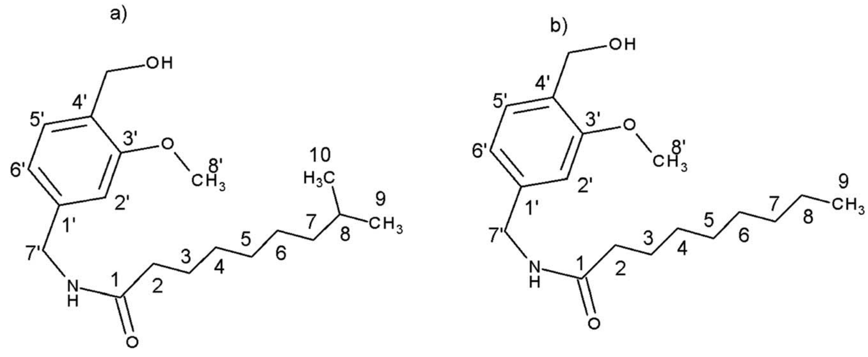

Fig. 1 Structure of (a) dihydrocapsaicin (DHCAP) and (b) nonivamide (NVA) with numbering of carbon atoms.

^{13}C CPMAS NMR spectroscopy

The ^{13}C and ^{15}N magic angle spinning (MAS) NMR spectra of solid samples were recorded on a Bruker DRX-400 Advance spectrometer using a Bruker PH MAS VTN 400WB BL4 probehead. Samples packed in a 4 mm ZrO_2 rotor were spun at 10 kHz (^{13}C) and 5 kHz (^{15}N). Contact time of 2.5 ms, repetition time of 10 s and spectral width of 20 kHz were used for accumulation of 200 scans for standard ^{13}C MAS experiments. For the acquisition of ^{15}N MAS spectra these parameters were: 5 ms, 10 s and 12 000 scans, respectively. ^{13}C chemical shifts were calibrated indirectly through the glycine CO signal recorded at 176.0 ppm, relative to TMS. ^{15}N chemical shifts were calibrated through the glycine NH signal δ ^{15}N 10.0 ppm and referenced to nitromethane δ $^{15}N = 380.2$ ppm (liquid NH_3 δ $^{15}N = 0$). Solid-state NMR cross-polarization (CP) ^{1}H–^{13}C experiments were performed with contact times in the range from 25 μs to 18 ms.

Genetic algorithm

A conformational search was carried for each molecule using genetic algorithm (GA) with multimodal optimization. Special software (ALJAR05) was developed for the calculations and used as described earlier.[6] Each conformation was first optimized using molecular mechanics (MMFF94 force field) to classify the conformers found by the genetic algorithm methodology.

GIAO DFT calculations

Further calculations of NMR shielding constants were performed using the DFT method with the B3LYP functional and the 6-311G(d,p) basis set (Gaussian 09 software[7]). Values of chemical shifts for each conformation were obtained in two ways: (i) by calculating TMS carbon atoms shielding constants and using the equation $\delta_{iso} = \sigma_{TMS} - \sigma_{iso}$ and (ii) by converting shielding constants with scaling factors.[8] The model conformers were

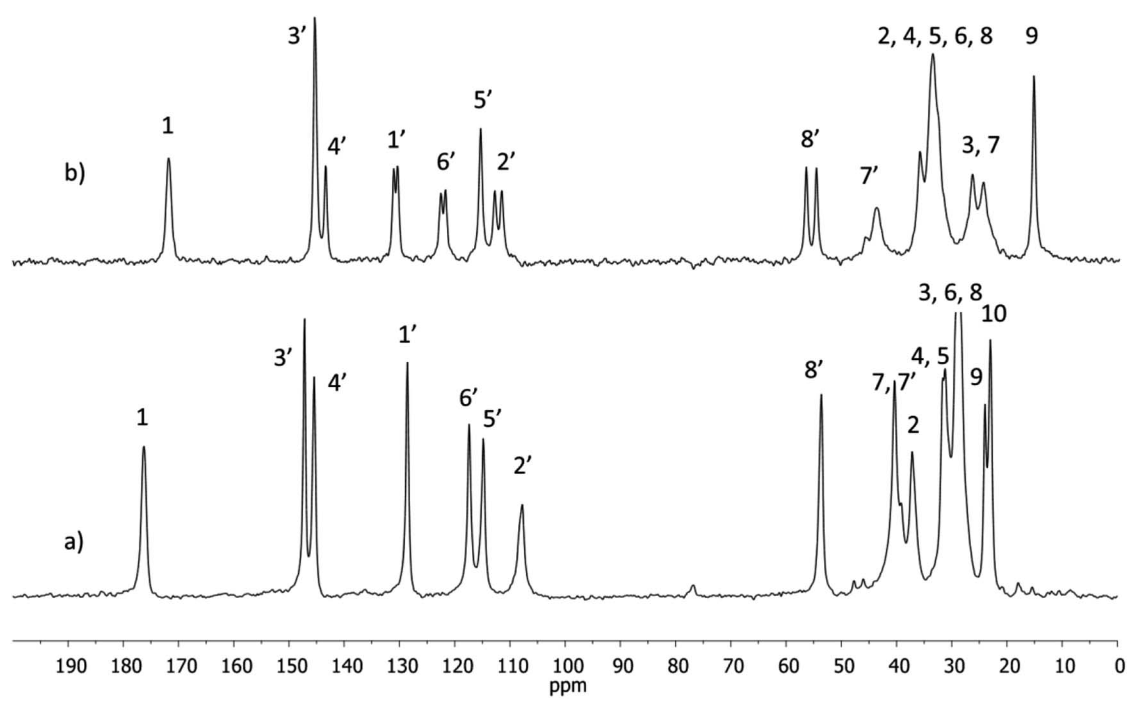

Fig. 2 ^{13}C CPMAS NMR spectra of (a) DHCAP and (b) NVA.

verified by comparing calculated shielding constants with experimental MAS NMR chemical shifts. For ^{15}N NMR, the reference molecule nitromethane was also optimized and its isotropic NMR shielding constants were calculated.

Results and discussion

^{13}C CPMAS NMR

^{1}H and ^{13}C NMR spectra of NVA and DHCAP (in $CDCl_3$ solutions) were measured and assigned. The chemical shifts were in agreement with those reported previously by Gómez-Calvario *et al.*[9] ^{13}C CPMAS NMR spectra were recorded for both solids and are illustrated in Fig. 2.

Resonances in the solid-state spectra were assigned by comparison with liquid-state chemical shifts and the results are collected in Table 1.

The ^{13}C signals in the solid-state spectrum of DHCAP were assigned first on the basis of liquid-state chemical shifts and the results are collected in Table 1. The assignments were further confirmed by the calculation of shielding constants. The signals of carbons C1 and C7′ bound to nitrogen might be slightly broader due to the interaction with quadrupolar 14 N nuclei but the effect was not observed in the spectra recorded with spinning speed of 10 kHz. Significant differences between chemical shifts in solution and solid state ($\Delta = \delta_{sol} - \delta_{ss} > 1.5$ ppm) are observed for both compounds, but for different carbon atoms.

For DHCAP, the differences appear for aromatic carbons C1′, C2′, C6′ and also for C7′and C8′. Similar differences were noticed earlier for capsaicin.[5] All three neighbors of C1′ exhibit an increase of shielding (3.4–3.8 ppm) in the solid state, suggesting the presence of steric hindrance. Molecular modeling shows that the rotation about C1′–C7′ bond is crucial and results in intramolecular interactions of C7′–H with either C2′–H or C6′–H. Significant values of Δ may be due to the locking of this fragment into a particular conformation, for example one of the C7′–H located closer to C6′–H and OCH_3 group near aliphatic chain (Fig. 1).

Considering the NVA molecule, the most remarkable differences in chemical shifts (*ca.* −4.5 ppm) are observed for methylene carbons C4, C5 and C6 of the chain. The signals of four aromatic carbons (1′, 2′, 3′, 6′) and OCH_3 (C8′) appear as doublets. The presence of split resonances indicates that two different molecules coexist in an asymmetric part of a unit cell of solid NVA. An attempt to assign the resonances to particular conformer was made. It is possible that one of them is similar to DHCAP, with OCH_3 group near aliphatic chain as suggested by comparable values of Δ. But for the second conformer these differences are smaller suggesting that this molecule has aliphatic chain oriented far from aromatic ring and therefore may be less hindered.

On the basis of ^{13}C CPMAS NMR and theoretical B3LYP/6-31G** calculations we could characterize the structure of conformers in solid phase. The chemical shifts for some conformers with different orientations of aliphatic chain, hydroxy and methoxy groups have been calculated by GIAO DFT. In solids, the rotation of hydroxy and methoxy groups is usually frozen, revealing specific environments with different chemical shifts, best seen for aromatic carbons *ortho* to the substituent. Better correlations between the measured and the calculated δ_{ii} values confirmed the existence of conformers with "anticlockwise" orientation of OH and OCH_3 groups, *e.g.* with OCH_3 pointing to C2′ and OH towards OCH_3 oxygen (Fig. 1).

Besides conformational effects, ^{13}C CPMAS chemical shifts reflect intermolecular interactions in solids. The formation of H-bonds results in changes of the chemical shift (deshielding) of carbonyl carbons. In $CDCl_3$ only weak interactions with the solvent occur, whereas in the solid state the C═O···HN and/or

Table 1 ^{13}C NMR chemical shifts of NVA and DHCAP in $CDCl_3$ (δ, ppm, ref. TMS) (δ_{sol}), solid-state (δ_{ss}) and differences $\delta_{sol} - \delta_{ss} > 1.5$ ppm

DHCAP				NVA			
C atom no.	δ_{sol}	δ_{ss}	Δ	C atom no.	δ_{sol}	δ_{ss}	Δ
1′	130.82	128.59	2.23	1′	129.94	130.48/131.14	
2′	111.19	107.77	3.42	2′	110.74	111.66/112.92	—/−2.18
3′	147.22	147.19		3′	146.70	145.41	
4′	145.62	145.44		4′	145.19	143.46/145.41	1.73/—
5′	114.88	114.82		5′	114.37	115.48	
6′	121.23	117.39	3.84	6′	120.86	121.85/122.65	—/−1.79
7′	43.99	40.4	3.63	7′	43.76	43.9	
8′	56.39	53.6	2.76	8′	55.98	54.8/56.6	
1	173.38	176.3	−2.9	1	173.53	171.9	1.5
2	37.32	37.3		2	36.55	36.08	
3	26.30	28.7	−2.3	3	25.88	26.58	
4	29.85	31.5	−1.6	4	29.29	33.75	−4.46
5	30.11	31.6	−1.5	5	29.14	33.75	−4.61
6	27.72	28.7		6	29.14	33.75	−4.61
7	39.43	40.4		7	22.63	24.58	−1.95
8	28.41	28.7		8	31.79	33.75	−1.96
9	23.10	24.0		9	14.08	15.46	
10	23.10	23.0		—	—	—	—

C=O···HO bonds should affect the δ_{ss} value. In DHCAP, chemical shift of C1=O for solution is 173.38 ppm, and for solid state 176.28 ppm. The deshielding ($\Delta = 2.9$ ppm) confirms the formation of intermolecular hydrogen bonds. For NVA, the difference of chemical shift between solution and solid state is +1.5 ppm and an increase of shielding suggest absence of hydrogen bond-type interaction involving C=O group.

^{15}N MAS NMR

^{13}C CPMAS spectra of solid NVA and DHCAP indicate that DHCAP has only one molecule in an asymmetric part of a unit cell, whereas NVA may have two. ^{15}N MAS NMR spectra provide confirmation of these findings. In ^{15}N MAS NMR spectrum of DHCAP a narrow singlet appears at −259.3 ppm, whereas in the spectrum of NVA a doublet is visible at −257.2/−258.2 ppm (Fig. 3).

The value of ^{15}N chemical shift for both compounds is typical for aliphatic and aromatic amides.[10] In both solids, hydrogen bonds may be formed by the OH···O=C or NH···O=C interaction. The NH···O=C interaction should be reflected in ^{15}N MAS chemical shift. If DHCAP is stabilized by NH···O=C H-bonds, and NVA is not, their ^{15}N chemical shifts would be significantly different. The relationship between ^{15}N MAS chemical shift and hydrogen bond-type interactions *via* NH group has been previously described and the effect of H-bond formation is estimated as *ca.* 8 ppm.[11] The ^{15}N signals of DHCAP and NVA have almost the same chemical shift, values differ only by 1–2 ppm suggesting similar type of intermolecular interactions. Thus, one can assume that molecules of NVA and DHCAP are not linked by NH···O=C bonds. The deshielding of C=O in ^{13}C MAS spectrum of DHCAP can be explained rather by OH···O=C interactions.

GIAO DFT calculations were performed for an isolated molecule of DHCAP and NVA and the values of ^{15}N NMR chemical shift (−256.0 and −254.6 ppm, respectively) are in agreement with experimental data.

Cross-polarization dynamics

It seemed worth to check if DHCAP and NVA exhibit distinct cross-polarization dynamics. Therefore, a series of ^{13}C CPMAS spectra with various contact times were recorded. According to the classic I-S model[12] the signal intensity in CP spectra is a function of contact time t:

$$I(t) = A(1 - T_{CP}/T_{1\rho}^{H}) - 1[\exp(-t/T_{1\rho}^{H}) - \exp(-t/T_{CP})] \quad (1)$$

where A is the intensity amplitude. The progress of cross-polarization is characterized by the time constant T_{CP} and the decrease in intensity for longer contact times t is due to the effects of ^{1}H spin–spin relaxation in the rotating frame, $T_{1\rho}^{H}$. Both parameters are specific for functional groups and differ for protonated and quaternary carbons.[13] The values of T_{CP} and $T_{1\rho}^{H}$ for dihydrocapsaicin, capsaicin and nonivamide are given in Table 2. Selected spectra of DHCAP and NVA recorded with varying contact times, are illustrated in Fig. 4a and b.

T_{CP} is governed by dipolar coupling[12] and is long for carbons without adjacent hydrogens. Quaternary carbon atoms of DHCAP and NVA have average T_{CP} values of 0.87 and 0.7 ms respectively. T_{CP} for CH groups is shorter (0.42–0.51 ms). Assuming that the average value of 0.42 ms is typical for CH carbons (Table 2), then 0.20 ms should be expected for CH_2 and even lower value for CH_3. The values for methyl carbons of 0.32–1.62 ms are longer than those expected without intramolecular dynamics, evidencing that methyl groups are fairly mobile. T_{CP} increases with increasing mobility of the structural fragment bearing this carbon, and the fast rotation is typical for methyl groups.[14] In the ^{13}C CPMAS spectra of DHCAP separate signals of two methyl groups appeared, therefore we were able to characterize particular carbons. The values of T_{CP} are 1.58 and 1.65 ms for C9 and C10, respectively, indicating that their interaction with intra- or intermolecular does not differ.

Relaxation times $T_{1\rho}^{H}$ are influenced by the short-range spatial proximity between protons and also reflect molecular dynamics. It seemed interesting to check if the two molecules

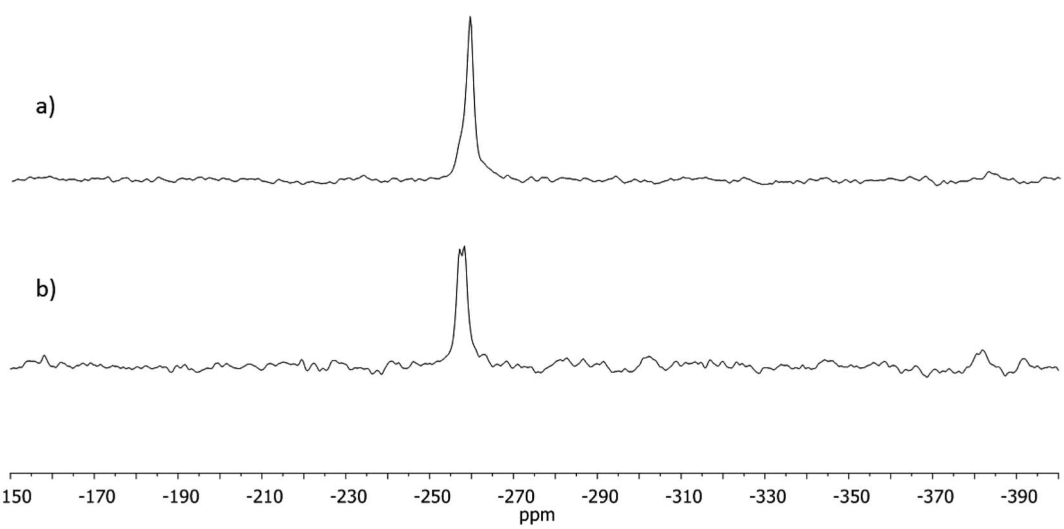

Fig. 3 ^{15}N MAS NMR spectra of (a) DHCAP and (b) NVA.

Table 2 Cross-polarization kinetic parameters: T_{CP} and $T_{1\rho}$ for dihydrocapsaicin, capsaicin[5] and nonivamide (nd – no data from cited publication)

Parameter	DHCAP Mean value ± SD [ms]	DHCAP Range of values [ms]	CAP[5] Mean value ± SD [ms]	CAP[5] Range of values [ms]	NVA Mean value ± SD [ms]	NVA Range of values [ms]
Quaternary carbons C1′, C3′, C4′						
T_{CP}	0.87 ± 0.24	0.65–1.13	0.95 ± 0.22	0.71–1.23	0.71 ± 0.08	0.64–0.80
$T_{1\rho}^{H}$	159 ± 15	143–172	154 ± 35	124–192	31 ± 8	24–40
T_{df}	0.95 ± 0.43	0.58–1.42	Nd	nd	0.87 ± 0.38	0.59–1.43
C1=O						
T_{CP}	0.69	—	0.67	—	1.14	—
$T_{1\rho}^{H}$	122	—	107	—	35	—
T_{df} (I-I*-S)	0.61	—	Nd	nd	0.52	—
C–H aromatic (C2′, C5′, C6′) and C8 in DHCAP						
T_{CP}	0.51 ± 0.09	0.45–0.65	0.42 ± 0.05	0.35–0.47	0.42 ± 0.08	0.33–0.49
$T_{1\rho}^{H}$	200 ± 58	150–250	149 ± 20	117–160	39 ± 7	35–48
T_{df} (I-I*-S)	0.42 ± 0.11	0.30–0.53	Nd	nd	0.29 ± 0.03	0.23–0.30
CH_2 (C2–C7) i C7′						
T_{CP}	0.38 ± 0.11	0.30–0.60	0.27 ± 0.12	0.2–0.47	0.20 ± 0.06	0.15–0.3
$T_{1\rho}^{H}$	148 ± 23	128–180	129 ± 15	115–148	23 ± 4	21–33
T_{df} (I-I*-S)	0.35 ± 0.11	0.20–0.50	Nd	nd	0.10 ± 0.09	0.05–0.31
CH_3 groups						
T_{CP}	1.62 ± 0.05	1.58–1.65	0.85 ± 0	—	0.32	—
$T_{1\rho}^{H}$	160 ± 14	150–170	160 ± 14	150–170	31	—
T_{df} (I-I*-S)	2.00 ± 0.00	2.00	Nd	nd	0.23	—
OCH_3 groups						
T_{CP}	0.68	—	0.45	—	0.50	—
$T_{1\rho}^{H}$	180	—	180	—	35	—
T_{df} (I-I*-S)	0.30	—	Nd	nd	0.32 ± 0.01	0.31–0.33

present in an asymmetric part of a unit cell of solid NVA exhibit distinct cross-polarization dynamics. Inspection of the spectra in Fig. 4, in which the doublets (C2′, C3′, C6′) of almost equal intensity are seen, as well as an analysis of T_{CP} and $T_{1\rho}^{H}$ values indicated that the behaviour of these two conformations is quite similar.

Fig. 5 shows the plot of signal intensity *vs.* contact time for methyl groups of NVA and DHCAP. Two signals of OCH_3 groups in NVA are characterized by long decay, similar to DHCAP. The $T_{1\rho}^{H}$ values obtained for CH_3 groups (both from the aliphatic chain and methoxy groups) are the same for DHCAP and CAP.

The plot of signal intensity *vs.* contact time for carbonyl carbons C1 is illustrated in Fig. 6; the shape of fitted functions is distinct: steeper for NVA and plane for DHCAP.

Unfortunately, no reliable data on cross-polarization dynamics can be provided on particular methylene carbons (except C7′) because of signal overlapping.

It is difficult to predict in advance which model will be better for the quantification of a particular CP signal. Therefore, we decided to analyze CP data in accordance with the I-I*S model. Intensity decays were described by Kolodziejski and Klinowski[12] by the following equation:

$$I(t) = I_0[1 - \tfrac{1}{2}\exp(-t/T_{df}) - \tfrac{1}{2}\exp(-\tfrac{3}{2}t/T_{df})\exp(-\tfrac{1}{2}t^2/{T_2}^2)],$$

where T_{df} is the proton spin-diffusion constant. T_{df} values for DHCAP and NVA are collected in Table 2.

Relaxation time in the rotating frame is frequently averaged over all protons by spin diffusion and is indicative for separation of molecules or some domains (*e.g.* aliphatic and aromatic) by missing intimate spin contact. T_{df} are long for quaternary carbon atoms. C4′ and C3′ which are the most distant from aliphatic chain carbon atoms have the longest T_{df} (0.85 and 1.42 ms for DHCAP, 0.82 and 1.42 ms for NVA, respectively). There are no significant differences in T_{df} values for aromatic ring carbon atoms. However, the CH_3 groups of the aliphatic chain of DHCAP and NVA differ in proton spin-diffusion constant. Methyl groups of DHCAP require longer spin-diffusion, which may be caused by fast rotation of isopropyl chain termination, as it was described earlier for CAP.[5] Shorter T_{df} value indicates that the CH_3 group of NVA may be less rotating. The average relaxation times in the rotating frame for solid capsaicinoids decrease in the order: DHCAP > CAP > NVA. Although the differences may be the result of different phenomena, including intramolecular mobility and intermolecular interactions, the

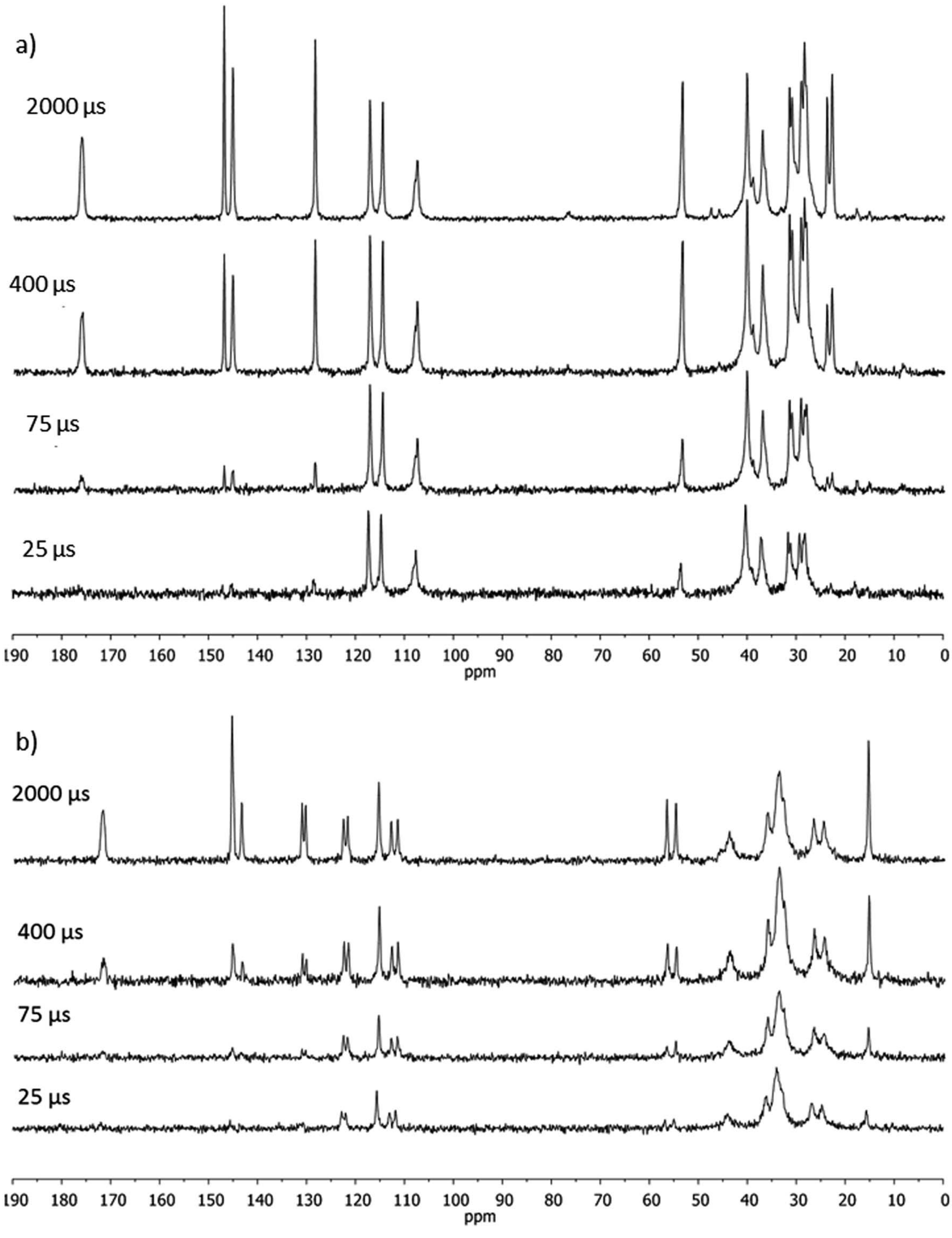

Fig. 4 ^{13}C NMR spectra of (a) DHCAP and (b) NVA, recorded with variable CP contact times.

lowest values for NVA (Table 2) suggest that solid NVA is more tightly packed and the chain has less space for dynamics.

$T_{1\rho}^{H}$ relaxation times are considered to be a probe of crystallinity degrees. For crystalline samples, $T_{1\rho}^{H}$ takes longer values than for amorphous samples.[15] It may suggest that NVA has a more disordered network compared to DHCAP and CAP. However, line broadening characteristic for amorphous solids is not observed neither in DHCAP nor NVA ^{13}C CPMAS spectra.

Cross-polarisation dynamic parameters were analyzed for the common pharmaceutical excipients.[15] Branched polymers of cellulose (methylcellulose, ethylcellulose, hydroxypropylmethylcellulose) have mean $T_{1\rho}^{H}$ value of 20 ms, which is similar to NVA. For some crystalline compounds, $T_{1\rho}^{H}$ values

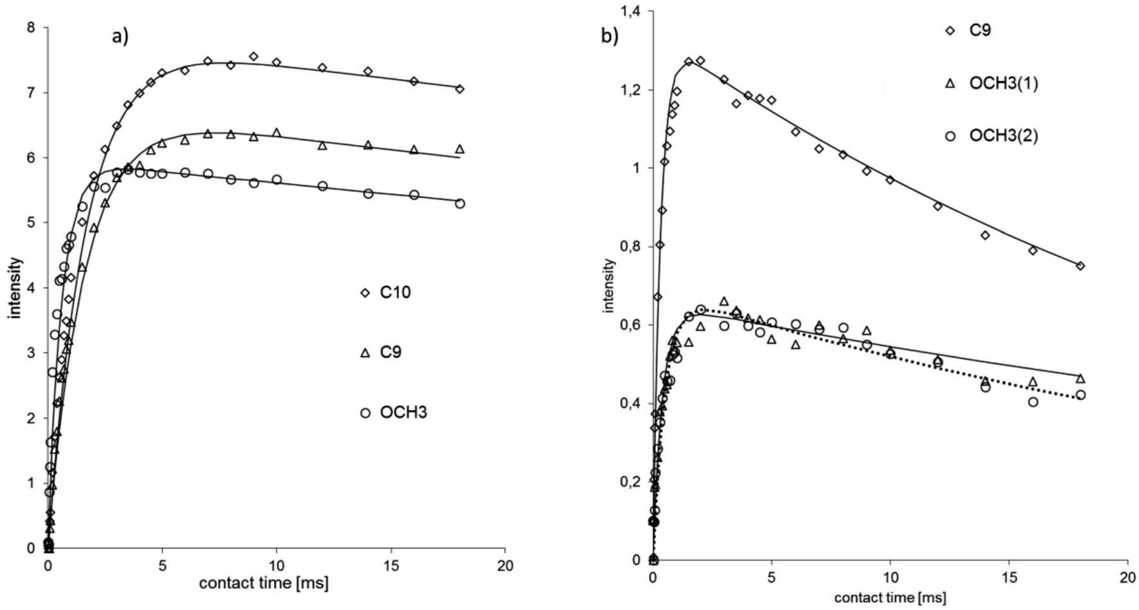

Fig. 5 Cross-polarization kinetics for methyl carbons of (a) DHCAP and (b) NVA. Signal intensity in arbitrary units (a.u), contact time in ms. The fitted functions have long $T_{1\rho}^{\mathrm{H}}$.

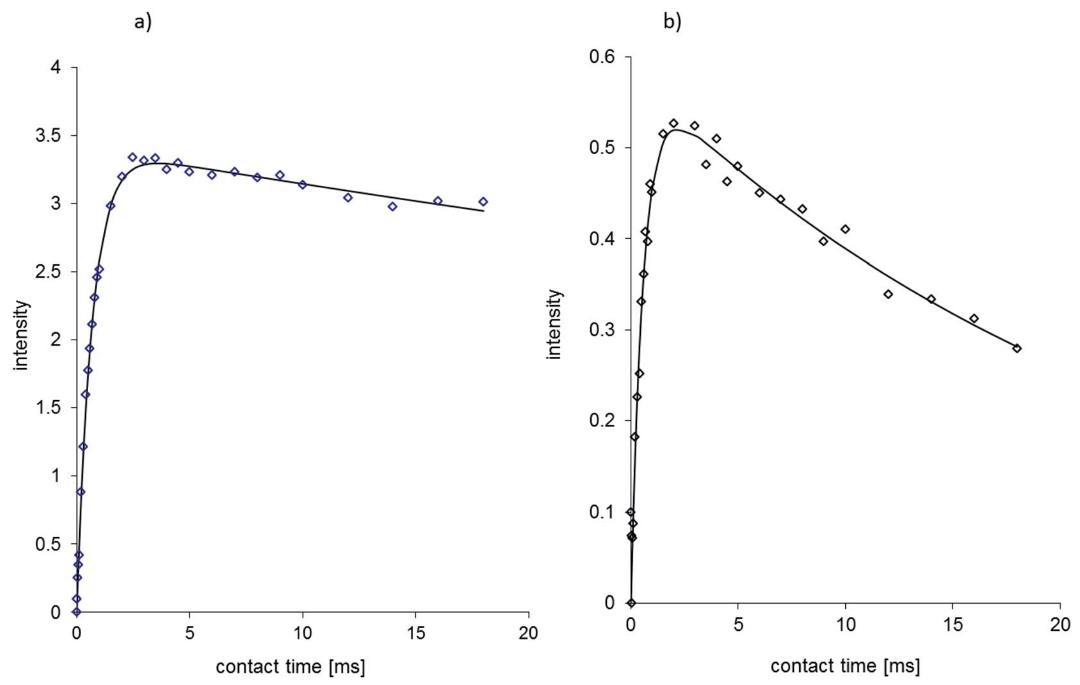

Fig. 6 Cross-polarization kinetics for C1=O carbon of (a) DHCAP and (b) NVA. The fitted functions have different $T_{1\rho}$ values. Signal intensity in arbitrary units (a.u), contact time in ms. Fitting using eqn (1) gives $T_{1\rho}^{\mathrm{H}} = 122$ ms for DHCAP and 35 ms for NVA. ($T_{\mathrm{CP}} = 0.61$ ms and 0.52 ms, respectively).

were significantly higher, for example olanzapine form II ($T_{1\rho} = \infty$).[16] The molecular dynamics of solid β-carotene were studied by means of ^{13}C CPMAS NMR.[17] The T_{CP} average value of 0.79 ms was found for methine carbons and 0.65–0.78 ms for methylene carbons, which indicated that these groups must be in a flexible molecular fragment. The relaxation times $T_{1\rho}^{\mathrm{H}}$ were very long (the CP curves ended in a plateau).

Genetic algorithm search

Low-energy conformations for NVA and DHCAP should be found for further molecular modelling, and simple DFT optimization is not efficient enough. For flexible compounds like NVA and DHCAP, systematical conformational searching (grid search) is extremely time consuming and is not recommended. A relatively new methodology of conformational analysis

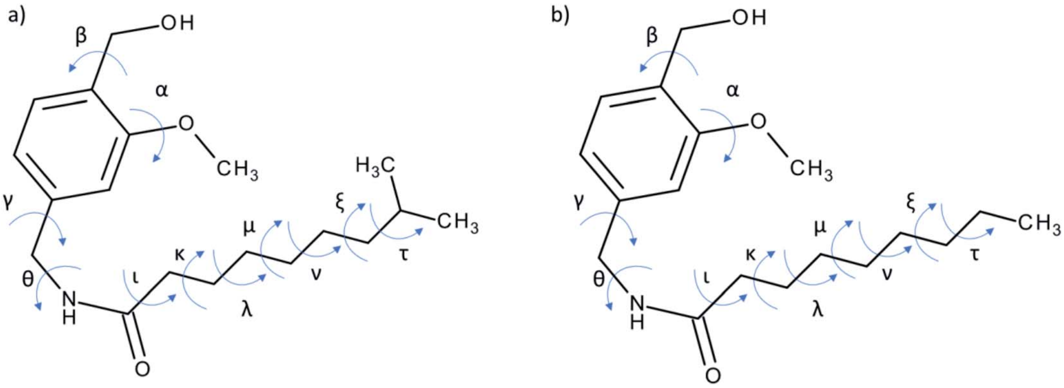

Fig. 7 Torsion angles of (a) DHCAP and (b) NVA selected for GA calculations.

Table 3 Chemical shifts calculated by GIAO DFT for selected DHCAP conformers from GA (R^2-tail shows correlation to experimental ^{13}C CPMAS data of aliphatic chain carbons, E1, E4 – dielectric constants, 01, 02… – conformer number)

	E1-01	E1-03	**E1-04**	E1-06	E1-08	E4-01	E4-03	E4-05	**E4-07**	E4-08
C1′	141.00	141.30	**139.14**	141.05	140.92	140.99	140.38	141.28	**138.10**	140.73
C2′	116.36	116.14	**113.71**	116.24	115.31	116.76	117.99	115.89	**114.13**	115.86
C3′	154.14	154.43	**154.27**	154.17	154.69	154.49	154.20	154.25	**152.45**	154.14
C4′	155.12	153.41	**155.19**	155.27	155.25	154.99	153.91	154.71	**154.56**	155.81
C5′	118.71	118.49	**119.79**	119.66	119.65	119.40	119.15	118.97	**121.57**	119.18
C6′	126.56	126.38	**128.08**	126.62	126.56	126.75	126.73	126.38	**128.23**	126.32
C7′	47.81	47.82	**46.29**	47.87	47.54	47.79	48.89	47.63	**48.47**	47.44
C8′	57.37	57.07	**56.80**	56.92	56.39	57.54	57.07	57.28	**57.03**	56.95
C1	178.39	178.72	**176.74**	179.03	178.31	178.35	179.22	178.90	**177.29**	178.91
C2	42.16	43.16	**40.68**	36.32	38.94	41.99	41.46	43.02	**43.00**	39.77
C3	34.10	33.31	**30.74**	25.75	24.80	34.29	28.80	30.48	**32.87**	26.14
C4	34.26	34.95	**31.90**	31.16	29.05	32.42	38.73	35.93	**34.17**	29.59
C5	37.70	36.82	**31.19**	27.95	30.45	36.32	35.51	36.08	**36.34**	29.55
C6	34.50	33.98	**30.87**	28.98	28.10	33.48	36.24	32.79	**32.90**	28.04
C7	44.88	43.10	**39.72**	43.15	41.59	42.48	44.50	45.62	**45.02**	41.67
C8	36.04	36.59	**29.77**	31.45	36.65	36.82	36.02	36.45	**35.62**	36.34
C9	22.14	26.44	**20.89**	20.79	22.17	22.69	26.42	26.34	**22.51**	22.02
C10	26.98	22.58	**26.71**	26.50	26.99	26.31	22.28	22.30	**28.45**	26.87
R^2-tail	0.907	0.878	**0.924**	0.841	0.723	0.857	0.822	0.911	**0.934**	0.758

capable of locating minimum energy structures on conformational potential energy surfaces are evolutionary algorithms (GA) based on the concepts of biological evolution. A 'population' of possible solutions to the problem is first created with each solution being scored using a 'fitness function' that indicates how good they are. The population evolves over time and allows you to receive better solutions. Of the various types of evolutionary algorithm, the genetic algorithm (GA) is the most well-known. The idea of GA is based on the genetic principles of heredity transferred to the field of quantum chemistry. The best adapted, low-energy conformations are selected and promoted to the next generations.

In our research for DHCAP and NVA 11 torsion angles were defined (Fig. 7) and listed in Table 5. The GA calculations with MMFF94 force field were carried out using two different dielectric constants ($\varepsilon = 1.0$, $\varepsilon = 4.0$). The higher ε value mimics the more polar surrounding of the molecule. The purpose was to verify how electrostatic interactions affect the optimal arrangements of the aliphatic chain. A set of low-energy conformers was obtained differing by *ca.* 1 kcal mol^{-1} (genetic algorithm procedures yielded *ca* 30 low-energy conformers for each compound). Then shielding constants calculation was carried out using DFT methods[7] for each conformation. The calculated NMR shielding constants were converted into chemical shifts, allowing easier comparison with experimental data. The next step was to verify the agreement between experimental solid-state and theoretical NMR data (mainly in aliphatic chain region). Selected results are collected in Tables 3 and 4.

For each dielectric constant the best conformation was chosen (based on R^2-tail values). Energies and dihedral angles of selected conformers are listed in Table 5.

Shielding constants are usually recalculated to chemical shifts by comparison to theoretical shielding constant of TMS ($\delta_{iso} = \sigma_{TMS} - \sigma_{iso}$). However, there is a number of publications describing the converting of shielding constants with scaling

Table 4 Chemical shifts calculated by GIAO DFT for selected NVA conformers from GA (R^2-tail shows correlation to experimental ^{13}C CPMAS data of aliphatic chain carbons, E1, E3 – dielectric constants, 01, 02… – conformer number)

	E1-01	E1-03	E1-04	E1-05	E1-10	E4-04	E4-07	E4-08	E4-09	**E4-10**
C1′	**140.99**	141.27	140.79	141.18	140.90	141.21	140.90	142.68	141.18	**138.04**
C2′	**115.88**	116.82	116.58	117.02	115.86	117.33	114.92	118.60	117.02	**115.11**
C3′	**154.53**	154.78	154.59	154.17	154.15	154.06	154.50	156.75	154.17	**152.85**
C4′	**154.61**	155.17	154.29	154.42	155.61	154.68	154.60	153.71	154.42	**154.59**
C5′	**119.04**	119.62	119.17	119.08	119.58	119.24	119.50	117.94	119.08	**121.82**
C6′	**126.69**	126.79	126.66	126.78	126.61	126.58	127.07	124.18	126.78	**129.16**
C7′	**48.03**	48.03	48.24	47.76	47.39	48.21	47.29	47.78	47.75	**49.21**
C8′	**57.71**	57.37	57.33	57.07	56.84	57.32	57.23	57.04	57.07	**56.93**
C1	**179.05**	178.74	178.54	178.76	179.17	178.80	177.68	178.42	178.76	**176.89**
C2	**37.60**	42.58	41.97	42.71	41.93	42.14	40.95	41.87	42.71	**43.12**
C3	**30.26**	31.40	34.13	30.73	34.14	34.34	27.35	33.66	30.74	**31.13**
C4	**32.45**	30.13	30.93	29.08	34.92	32.35	28.71	32.11	29.08	**35.98**
C5	**34.84**	34.33	30.24	34.55	33.50	35.75	30.22	36.14	34.55	**35.81**
C6	**37.63**	31.74	28.10	28.27	31.21	36.48	29.08	35.52	28.27	**36.03**
C7	**39.32**	34.84	30.49	32.91	34.37	36.82	31.74	36.78	32.91	**39.29**
C8	**29.46**	30.07	21.62	27.95	23.59	30.13	26.48	30.16	27.95	**29.73**
C9	**16.84**	16.60	13.40	14.57	13.16	16.49	17.25	16.77	14.57	**17.69**
R^2-tail	**0.914**	0.787	0.653	0.733	0.813	0.902	0.753	0.866	0.733	**0.947**

factors (SF).[18,19] Empirical scaling enables achieving high-accuracy theoretical chemical shifts. In this approach, the systematic error was decreased by scaling factors determined *via* linear regression analyses of experimental and computed chemical shift data. It was proposed as a rewarding method.

The selected low-energy conformers (Fig. 8) differ mainly in the geometry of the aliphatic chain. Their isotropic ^{13}C shielding constants σ_{iso} were compared with the experimental $\delta_{CPMAS\ NMR}$ values. The correlation of the calculated isotropic shielding with each set of resonances in the MAS spectrum is satisfactory because $R^2 > 0.99$. As a criterion of the quality of conformers, the R^2 factor and the minimal absolute error (MAE) between theoretical and experimental data can be applied. However, the R^2 criterion used to determine the quality of fitting is not sensitive enough to make selection, therefore R^2-tail (which compares only the aliphatic chain carbons chemical shifts) and MAE were added as rewarding parameters. For both molecules, the two best conformations were chosen for each method of chemical shift conversion: DHCAP-E1, DHCAP-E4 and NVA-E1, NVA-E4 (see Tables 3 and 4).

The differences between chemical shifts calculated according to the TMS shielding constant and using scaling factors are visible at the first sight. The MAE is lower for these obtained by SF almost by half. The traditional approach in NMR calculations is calculating shielding constants for a reference molecule.[20] However, the utilizing of a single molecule reference compound may lead to a systematic error. In the case of SF, isotropic shielding constants are plotted against known experimental chemical shifts for a numerous set of small organic molecules.[21] and a strong linear correlation was observed.

The traditional approach, *e.g.* calculations of the isotropic shielding constant of TMS, allowed the selection of the best conformations: DHCAP-E1 and NVA-E1. DHCAP-E1 fulfils both criteria: the highest R^2-tail value (0.924) and the lowest MAE (4.08). For NVA the highest R^2-tail (0.933) and the lowest MAE (4.53) were also obtained for E1. However, when scaling factors were used, the best results were obtained for calculations with $\varepsilon = 4.0$. The R^2-tail was 0.934 and 0.910 and MAE 2.00 and 1.45 for DHCAP-E4 and NVA-E4, respectively. These four low-energy conformers, which show the best agreement between theoretical and experimental chemical shifts, are illustrated in Fig. 8. The aromatic part of DHCAP and NVA has the same structure in all conformers, with OCH_3 group pointing to C2′ and OH directed to oxygen at C3′. The most interesting structural part of both studied molecules is the flexible aliphatic chain.

Both GA-conformers of DHCAP have a bent chain, as it was found earlier for capsaicin.[5] However, in one of them it is bent

Table 5 Torsional angles and energy values (kcal mol^{-1}) calculated with MMFF94 force field at two different dielectric constants ($\varepsilon = 1.0$, $\varepsilon = 4.0$) obtained by GA for the low-energy conformers of DHCAP and NVA

Torsion angle	DHCAP-E1	DHCAP-E4	NVA-E1	NVA-E4
α (°)	−0.5	1.5	−0.9	1.8
β (°)	−0.4	0.4	−0.4	0.5
γ (°)	−69.6	118.2	−75.2	112.7
θ (°)	125.2	146.7	93	155.9
ι (°)	146.3	97.5	137.7	−133.5
κ (°)	−67.8	66.7	−67.6	−174.8
λ (°)	−177.5	176	−66.8	−177
μ (°)	178	66.5	−176.9	−66.3
ν (°)	64.5	176	179.9	−176.4
ξ (°)	60.7	175.3	−179.7	−180
τ (°)	60.1	63.8	−179.9	−179.8
ΔE	1.28	2.43	0.08	1.1
R^2	0.997	0.997	0.999	0.999
R^2-tail	0.924	0.934	0.914	0.947
MAE (TMS)	4.08	5.34	4.53	4.87
MAE (SF)	2.62	2.00	1.86	1.45

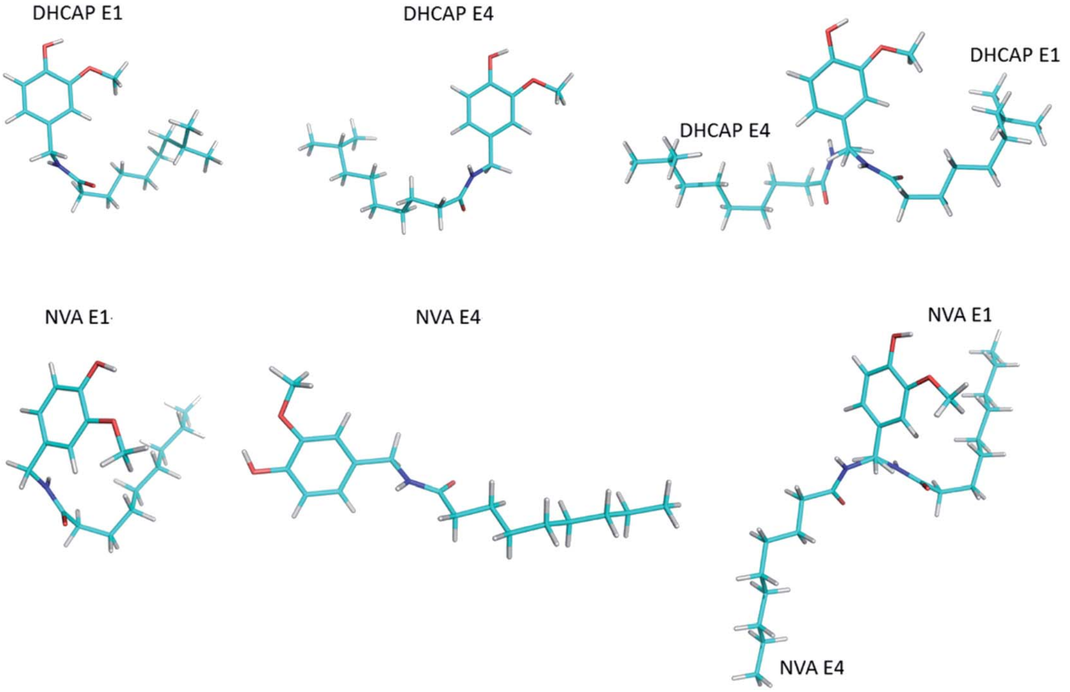

Fig. 8 The selected low-energy conformers of DHCAP and NVA and their overlapped structures.

towards the methoxyl group (E1), which may cause steric hindrance, whereas in the second – in the opposite direction (E4). The hindrance should influence the CP kinetic parameters. The CP parameters of DHCAP for both CH_3 and OCH_3 group are longer than CP parameters of CAP. It may suggest increased mobility of these groups, which is possible in the absence of the steric hindrance (E4). Summarized GA and CPMAS NMR data recommend that the most probable conformation of DHCAP is DHCAP E4. It is bent as capsaicin conformation, but in the opposite direction.

Both GA conformers of NVA, which have the best fitting parameters to experimental NMR data, have different geometries of aliphatic chain. The NVA-E1 has a bent and the NVA-E4 extended aliphatic chain. Split resonances (doublets) in ^{13}C and ^{15}N MAS NMR spectra suggest that solid NVA sample contains two different molecules in the crystallographic unit. Taking into account the conformers obtained by GA, we suppose that the molecules coexisting in the solid may differ by the orientation of aliphatic chain. However, to confirm such assumption crystallographic data are required.

Conclusions

The solid-state structure of DHCAP and NVA were investigated. Since there is no crystallographic data and single crystals suitable for XRD were not obtained, ^{13}C and ^{15}N MAS NMR supported by genetic algorithm and GIAO DFT calculations were used for solid state structural studies. To the best of our knowledge this work is the first that focuses on solid state of DHCAP and NVA. DHCAP shows numerous similarities in NMR and GA data to these obtained for CAP.[5] Conformation with a bent aliphatic chain is probable in solid DHCAP, however the chain is not close to the methoxyl group. The molecular network of capsaicinoids is not stabilized by NH···O=C intermolecular hydrogen bonds, more probable is OH···O=C interaction in DHCAP and CAP but not in NVA. Solid state of NVA is characterized by the presence of two conformers, with bent and extended aliphatic chain.

Conflicts of interest

There are no conflicts to declare.

References

1 K. Srinivasan, Biological activities of red pepper (Capsicum annuum) and its pungent principle capsaicin: a review, *Crit. Rev. Food Sci. Nutr.*, 2016, **56**(9), 1488–1500.
2 S. Kosuge and M. Furuta, Studies on the pungent principle of capsicum: part XIV chemical constitution of the pungent principle, *Agric. Biol. Chem.*, 1970, **34**(2), 248–256.
3 H. L. Constant, G. A. Cordell and D. P. West, Nonivamide, a constituent of capsicum oleoresin, *J. Nat. Prod.*, 1996, **59**(4), 425–426.
4 N. O. Junior, *et al.*, Evaluation of Natural Capsaicin (N. Cap) in Pepper Spray by GC-MS/FID, NMR and HPLC as an Alternative to the Use of Oleoresin Capsicum (OC), *Human Factors and Mechanical Engineering for Defense and Safety*, 2019, **3**(1), 1–10.
5 P. Siudem, K. Paradowska and J. Bukowicki, Conformational analysis of capsaicin using ^{13}C, ^{15}N MAS NMR, GIAO DFT and GA calculations, *J. Mol. Struct.*, 2017, **1146**, 773–781.

6 J. Bukowicki, A. Wawer and K. Paradowska, Conformational Analysis of Gentiobiose Using Genetic Algorithm Search and GIAO DFT Calculations with ^{13}C CPMAS NMR as a Verification Method, *J. Carbohydr. Chem.*, 2015, **34**(3), 145–162.
7 M. Frisch, *et al.*, *Gaussian 09, rev. B01*, Gaussian Inc., Wallingford CT, 2010.
8 M. W. Lodewyk, M. R. Siebert and D. J. Tantillo, Computational prediction of ^{1}H and ^{13}C chemical shifts: a useful tool for natural product, mechanistic, and synthetic organic chemistry, *Chem. Rev.*, 2011, **112**(3), 1839–1862.
9 V. Gómez-Calvario, *et al.*, ^{1}H and ^{13}C NMR data on natural and synthetic capsaicinoids, *Magn. Reson. Chem.*, 2016, **54**(4), 268–290.
10 M. Witanowski, L. Stefaniak and G. Webb, Nitrogen NMR spectroscopy, in *Annual reports on NMR spectroscopy*, Elsevier, 1993, pp. 1–82.
11 X. P. Xu and D. A. Case, Probing multiple effects on ^{15}N, ^{13}Cα, ^{13}Cβ, and ^{13}C′ chemical shifts in peptides using density functional theory, *Biopolymers*, 2002, **65**(6), 408–423.
12 W. Kolodziejski and J. Klinowski, Kinetics of cross-polarization in solid-state NMR: a guide for chemists, *Chem. Rev.*, 2002, **102**(3), 613–628.
13 U. Holzgrabe, B. W. Diehl and I. Wawer, NMR spectroscopy in pharmacy, *J. Pharm. Biomed. Anal.*, 1998, **17**(4–5), 557–616.
14 S. Witkowski, K. Paradowska and I. Wawer, ^{13}C CP/MAS NMR studies of vitamin E model compounds, *Magn. Reson. Chem.*, 2004, **42**(10), 863–869.
15 D. M. Pisklak, *et al.*, ^{13}C solid-state NMR analysis of the most common pharmaceutical excipients used in solid drug formulations part II: CP kinetics and relaxation analysis, *J. Pharm. Biomed. Anal.*, 2016, **122**, 29–34.
16 W. Kolodziejski, *et al.*, Kinetics of ^{1}H → ^{13}C NMR cross-polarization in polymorphs and solvates of the antipsychotic drug olanzapine, *Solid State Nucl. Magn. Reson.*, 2011, **39**(3–4), 41–46.
17 W. Kolodziejski and T. Kasprzycka-Gutman, ^{13}C CP/MAS NMR in trans-β-carotene, *Solid State Nucl. Magn. Reson.*, 1998, **11**(3–4), 177–180.
18 F. L. Costa, *et al.*, Very Fast and Surprisingly Accurate GIAO-mPW1PW91/3-21G//PM7 Scaling Factor for ^{13}C NMR Chemical Shifts Calculation, *Adv. Sci., Eng. Med.*, 2017, **9**(3), 254–261.
19 T. F. Giacomello, *et al.*, Protocol for Calculating ^{13}C Nuclear Magnetic Resonance Chemical Shifts of Flexible Organic Molecules, *Adv. Sci., Eng. Med.*, 2017, **9**(8), 640–647.
20 P. Wałejko, *et al.*, Racemic crystals of trolox derivatives compared to their chiral counterparts: structural studies using solid-state NMR, DFT calculations and X-ray diffraction, *J. Mol. Struct.*, 2018, **1156**, 290–300.
21 http://cheshirenmr.info/index.htm.

